

Coupled calculations COBAYA4/CTF for different MSLB scenarios in the frame of NURES SAFE project

S. Sánchez-Cervera¹, A. Sabater, D. Cuervo, N. García-Herranz

Department of Energy Engineering
Universidad Politécnica de Madrid (UPM)
José Gutiérrez Abascal 2, 28006, Madrid, Spain.
santiago.sanchezcervera@upm.es

Abstract – The new version of COBAYA diffusion code, COBAYA4, has been integrated into SALOME platform in order to enable the coupling with other thermal-hydraulics codes of the platform. Particularly, it has been coupled with CTF code, and the system COBAYA4-CTF is employed within NURES SAFE project for the simulation of MSLB transient in two different reactors: PWR and VVER.

I. INTRODUCTION

During the 7th Framework EURATOM NURES SAFE Project [Chanaron et al., 2015], in-depth modifications of the in-house COBAYA diffusion code have been accomplished at UPM. The main objective of this updating was to make possible its integration at nodal and pin level in the NUClear REactor SIMulation (NURESIM) SALOME platform [Chanaron, 2016] and its coupling with any other code of the platform for multi-physics analysis.

COBAYA is a multigroup neutron diffusion code developed at UPM able to perform nodal and pin-by-pin full core calculations in hexagonal and Cartesian geometry at different conditions, i.e. steady-state or space-time kinetics problems.

COBAYA3 was the consolidated version of the code after the 6th and 7th Framework European projects NURESIM and NURISP. After the modifications implemented during NURES SAFE project the code has evolved to COBAYA4.

The nodal solver employed in COBAYA [Lozano et al., 2008] is based on the Analytic Coarse-Mesh Finite-Difference method (ACMFD). It can be used either stand-alone or as an external acceleration for the Fine-Mesh Finite-Difference (FMFD) pin-by-pin solver. This last solver can perform full core calculations through domain decomposition techniques [Herrero, 2009] or using one calculation domain. The second method is suited in shared memory systems.

The process followed to integrate COBAYA4 in SALOME platform making use of the medcoupling structures is detailed in [García-Herranz et al., 2016]. The integration in SALOME enables the possibility to couple COBAYA4 component with other thermal-hydraulic (TH) codes such as CTF, FLICA4 or SUBCHANFLOW; and the coupling with CTF was performed during this project.

CTF is the improved version of COBRA-TF developed by the Reactor Dynamics and Fuel Management Group (RDFMG) from North Carolina State University under CASL consortium. CTF is a 3D core thermal-hydraulic code for LWR vessel and core analysis. It uses a two-fluid, three-

fields modeling approach and solves three momentum conservation equations, four mass conservation equations, and two energy conservations equations [Salko, 2015]. CTF is able to solve the TH problem at two levels, assembly averaged channel level and sub-channel level.

Thanks to the integration scheme, it is possible to carry out coupled calculations using different resolutions for the neutronic (NK) and the TH solvers. That means that a neutronics nodal or pin-by-pin calculation can be performed using TH channels (one per assembly) or TH sub-channels (one among four fuel pins). A study has been performed for a fuel assembly in [Sabater 2016] assessing the impact of using channel averaged or sub-channel in CTF.

The system COBAYA4-CTF has been employed in NURES SAFE project for the simulation of Main Steam Line Break (MSLB) scenarios. Particularly, a comparison between nodal and pin-by-pin solutions is performed for a PWR and a MSLB in a VVER is analyzed this work.

II. DESCRIPTION OF THE ANALYSES

Two benchmarks are designed to provide the framework to assess the ability of different codes integrated in SALOME platform to predict the transient response in a MSLB scenario. These benchmarks differ depending on the type of reactor.

For the PWR, the reference reactor is the four-loop Westinghouse of Zion NPP, which has been also used in other benchmarks [Kozłowski 2003]. The core configuration includes four different types of fuel assemblies: MOX and UOX, each with two different initial enrichments. Their geometries and initial compositions are given in [Kozłowski 2003].

In order to maximize the reactivity effect of the core overcooling due to the MSLB, the transient is assumed to start at the end of cycle (EOC) when the boron content is negligible and the Xenon concentration in the core is zero. The initial steady-state corresponds to the Hot Zero Power (HZIP) conditions and the transient is initiated from a subcritical state corresponding to a 1% SDM, All Rods In (ARI), with the highest worth control rod stuck in the

overcooled area. Detailed information of the transient can be found in [Kliem et al., 2016].

Since CTF is a TH code focused in the core (sub-channel code) it does not predict the response of the plant, so time-dependant boundary conditions have been provided by Helmholtz-Center Dresden-Rossendorf (HZDR) using ATHLET system code.

Two transient simulations have been performed: a NK nodal calculation (hereafter referred as nodal) and a NK pin-by-pin calculation (hereafter referred as PbP) using in both cases one TH channel per assembly. Cross-section libraries in both cases were generated using APOLLO2 lattice code and are fully consistent. They include, apart from two-group homogenized cross-section data, fuel assembly discontinuity factors and kinetic parameters.

Data are provided in NEMTAB-like format, that is, the data dependence on the state variables is specified through a multi-dimensional table look-up. COBAYA can then use a simple linear interpolation scheme to compute appropriate parameters at the required reactor conditions. To minimize the interpolation error, an optimisation process is used to set the grid of state variables values for branch calculations [Sánchez-Cervera, 2014]. This process refines the grid in the domain where keff is more sensitive to cross-section variation, which is assessed by computing adjoint-flux based sensitivity coefficients. The final state variables distribution is shown in Table I.

Table I. Optimized grid structure for the state variables (120 branch cases)

State-variable	Data-points
Moderator density (kg/m ³)	300 382.58 465.15 630.3 960.6
Doppler temperature (K)	373 779.75 1186.5 2000
Moderator temperature (K)	373 495 617
Boron concentration (ppm)	0 600

Concerning the VVER, the definition of the transient has been derived from OECD VVER-1000 MSLB benchmark [Kolev, 2010]. The reference core is Kozloduy-6 Cycle 8 which is composed by a classical three-batch equilibrium cycle.

The MSLB transient is initiated at HFP by a large break of steam line 4 upstream of the steam intercept valve, outside the containment. Following the break and the scram signal, two of the most reactive peripheral control assemblies remain stuck out of the core, close to the location of maximum overcooling. Two scenarios have been specified. Scenario 1 is realistic, as used in the current licensing practice. Scenario 2 is pessimistic, assuming that the main coolant pump (MCP) of the faulted loop fails to trip on MSLB signal and all MCP remain in operation during the transient. The scram worth in Scenario 2 is assumed to be artificially reduced to about 50% of the real

one by adjusting the absorption cross-sections in UOX-CR assemblies and by using this modified library. This allows for a significant return to power after scram in the 3D core NK/TH calculations, which is a good test for the coupling schemes. For transient simulation Scenario 2 is considered only.

The cross-section library was generated by INRNE also with APOLLO2 and it is available in two formats: compact and extended. The first one includes a correction in the down-scattering and discontinuity factors are implicitly included whereas the extended one provides them explicitly. Cross-sections are obtained for the state-points shown in Table II, which have been obtained applying the same optimization process than for the PWR. Notice that in this case the range of the moderator density is too broad so a high number of data-points is required.

Table II. Optimized grid structure for the state variables in VVER

Boron conc.(ppm)	Doppler T. (K)	Mod. Dens. (kg/m ³)	Mod.T. (K)
53	470	50	470
	852.5	76	545
	1235	102	620
	1617.5	128	
	2000	154	
		207	
		259	
		311	
		363	
		467.5	
		572	
		676	
		885	

III. PWR RESULTS

1. HZP Steady State

The initial state of the reactor core before the MSLB has been computed. A fixed value of 0.99 for the effective multiplication factor was set following the specifications.

Results are summarized in Table III, where values of power peaking factors are included. The pin-by-pin solution predicted an axial power peaking factor Fz 1.2% higher than the nodal solution whereas the radial factor Fxy, defined as the maximum axially-integrated radial power per assembly, is 4.3% lower. Also Fq factor is higher in nodal case than in pin-by-pin.

Pin-by-pin calculation provides more detailed information. For example, the radial pin peaking factor is 14% higher than the assembly-averaged one, which indicates that there is a strong peaked distribution in the hot assembly.

Fig. 1 shows the radial power distribution of the core (axially-integrated) for the PbP calculation, averaged on the

assembly. It is easy to identify the position of the stuck rod. Fig. 2 includes the relative differences respect to the nodal calculation and maximum differences are obtained in the part diametrically opposite to the part with the withdrawn rod.

Concerning time consumption, the pin-by-pin calculation took around 3 hours on a single Intel Core i7 at 3.07 GHz, while the nodal calculation took around 3 min. on the same core.

Table III. Results for HZP calculations

	COB4/PbP	COB4/nodal	Diff.
Fixed keff	0.9900	0.9900	
Axial power peaking factor (F_z)	1.96	1.93	-1.2%
Radial assembly peaking factor ($F_{xy_assembly}$)	7.67	7.93	4.3%
Radial pin peaking factor (F_{xy_pin})	8.77	-	-
Hot spot power peaking factor ($F_{q_assembly}$)	15.06	15.40	2.3%
Hot spot power peaking factor (F_{q_pin})	17.22	-	-

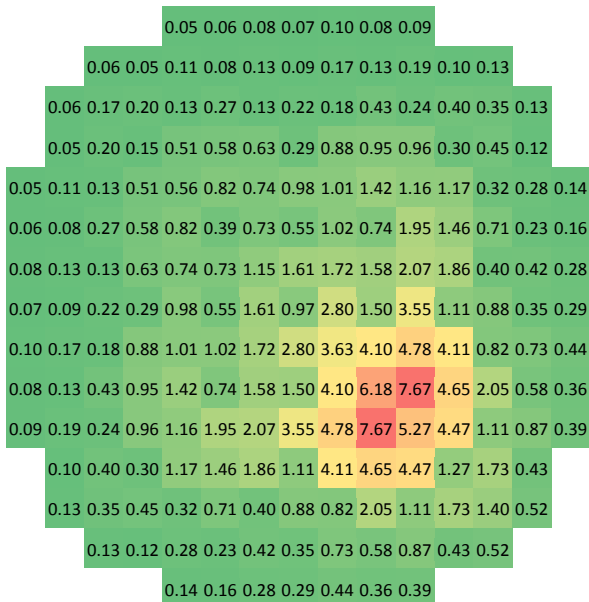


Fig. 1. Axially-integrated radial power distribution for the pin-by-pin calculation (averaged on the assembly)

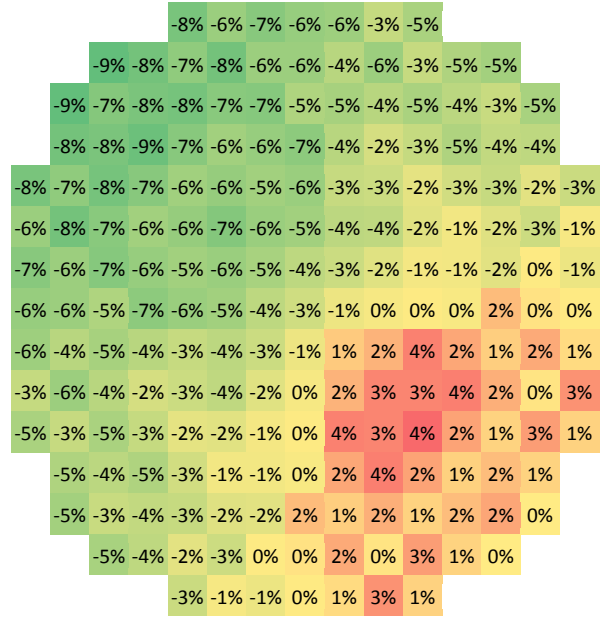


Fig. 2. Relative differences in percent of the distribution computed with a nodal calculation

2. Transient

Due to the overcooling caused by the MSLB event (occurring at 0 s), there is a positive reactivity insertion in the reactor dominated by a large negative temperature coefficient of the coolant. The evolution of the core reactivity is shown in Fig. 4. Starting from -1000 pcm, which corresponds to the fixed value in k-effective in the initial steady state, the reactivity increases. The change in the slope at ~15 s reflects the change in the water inlet temperature and mass flow rate produced by the closing of the Main Steam Isolation Valve (MSIV) in the steam generator. The time history of those variables, provided by ATHLET and taken as boundary conditions by COBAYA, is represented in Fig. 5 and 6.

The core reaches criticality at ~28 s and maximum overcriticality at ~40 s, when a power excursion takes place. The consequent increase in the fuel temperature (see Fig. 7) leads to a negative reactivity insertion due to Doppler feedback effect so that the core reactivity decreases progressively.

The evolution of the total power can be seen in Fig. 3. The initial power excursion is followed by a smoother rise, reaching a maximum value around 240 MW at 89 s. The delay between the core criticality and the sudden rise of power is explained by the time characteristics of the delayed neutrons, which determine the kinetic transient response since reactivity keeps always below 1\$. Detailed values are provided in Table IV.

Table IV. Comparison of parameters

	COBAYA4/PbP		COBAYA4/Nodal	
	Time (s)	Value	Time (s)	Value
Core criticality	28.5 s.	-	28	-
Max. reactivity	41	387.6 pcm	40.5	403.0 pcm
Max. core power	89	240.3 MW	88.5	236.6 MW
Return subcritic.	106.5	-	111	-

Both nodal and pin-by-pin solutions provide similar results. However, slight differences can be found. For example, the power excursion in PbP presents a ~1 s delay. When comparing peak factors the differences become higher. Fig. 8 shows the evolution of the radial assembly-averaged peaking factor F_{xy} and it can be checked that PbP solver predicts a lower solution than the nodal one during the whole transient

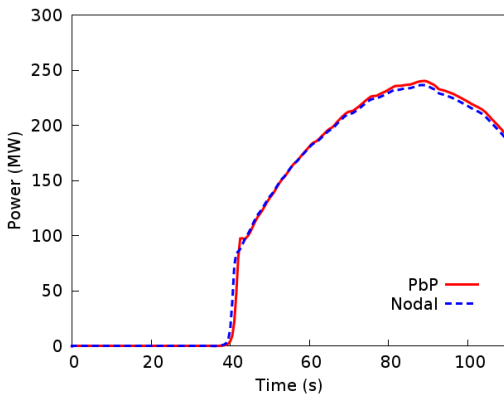


Fig. 3. Power evolution during the MSLB in a PWR

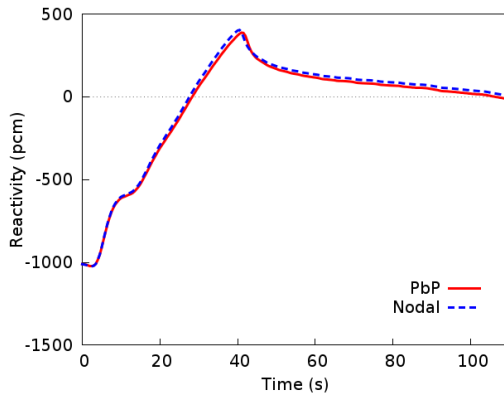


Fig. 4. Reactivity evolution during the MSLB in a PWR

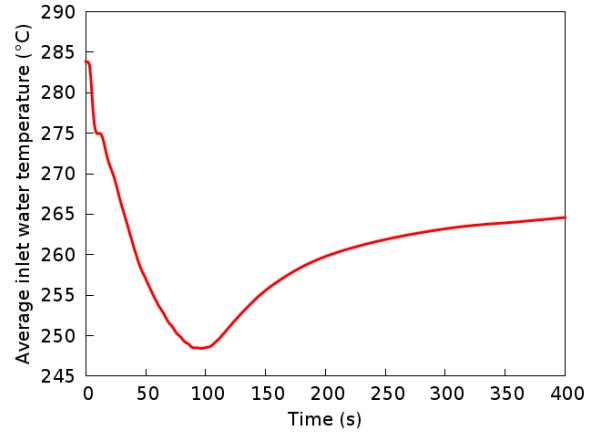


Fig. 5. Time history of the inlet water temperature (boundary condition)

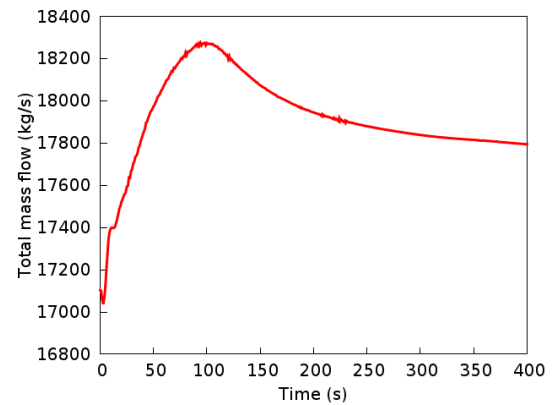


Fig. 6. Time history of the mass-flow

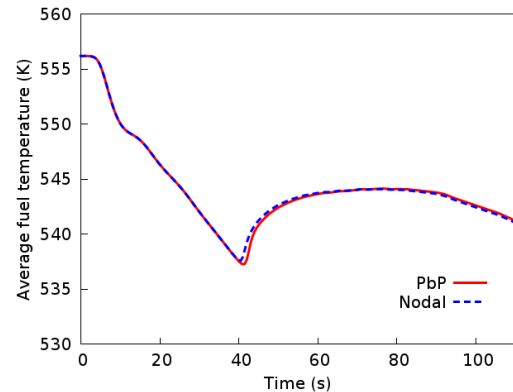


Fig. 7. Average fuel temperature during the MSLB in a PWR

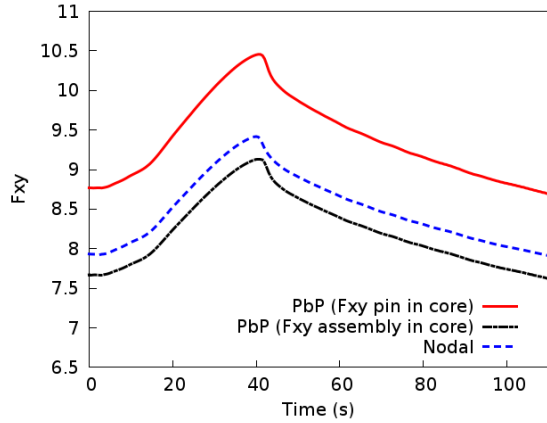


Fig. 8. Evolution of the radial peaking factor F_{xy} during the MSLB in a PWR

IV. VVER RESULTS

1. Steady State

According to [Kolev, 2016a] a set of states is defined, with different configurations of control rods banks and combining the two scenarios. These states are shown in Table V. Table VI includes the results obtained with COBAYA4 for the different HZP states and using the compact library. These results are in very good agreement with other codes such as DYN3D, as can be checked in [Kolev, 2016a]. The axial power distribution of one HZP case (case 0) is represented in Fig. 9. At HZP state the axial offset is positive, that is, the peak power is in the upper part of the core because there is no TH profile and there is more fissile material in this part due to the burnup of previous cycle.

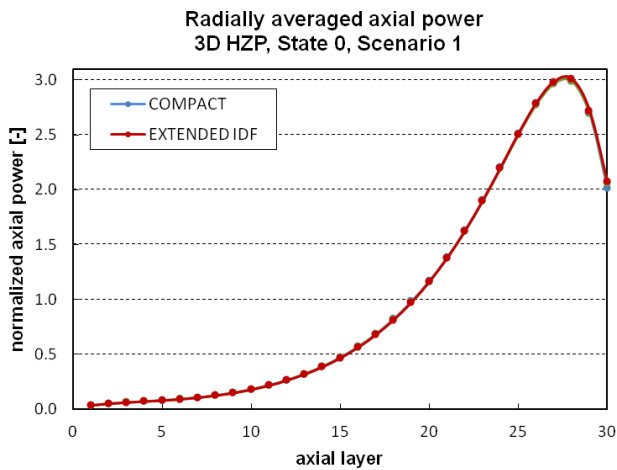


Fig. 9. Axial power distribution at HZP for VVER

Table V. Definition of steady-state cases

State	TH conditions	Control rod position	Scenario
0	HZP	Groups 1-10 ARO	1
1a	HZP	Groups 1-5 up, 6 -81% wd, 7-10 down	1
1b	HZP	Groups 1-10 ARI	1
2	HFP	Groups 1-9 ARO, 10 is 80% wd	2
3	HZP	Groups 1-10 ARI #90 is 100% wd	1
4	HZP	Groups 1-10 ARI #140 is 100% wd	2
5	HZP	Groups 1-10 ARI #117 & #140 are 100% wd	2

Table VI. Summary of COBAYA4 results at HZP states in VVER

State	k-eff	F_{xy}	F_z
0	1.02534	1.341	2.983
1a	0.98804	1.406	2.001
1b	0.94823	1.454	2.713
1b-sc2	0.99727	1.407	2.859
3	0.95709	8.354	2.323
4	0.99792	1.800	2.835
5	0.99891	2.504	2.801

HFP simulation is performed with compact and extended libraries and the axial distribution is shown in Fig. 10. In this case the profile is flatter than in HZP cases thanks to the TH profile. The distribution of the different variables can be plotted using SALOME platform. In Fig. 11 the axial and radial distributions of the moderator density, fuel temperature and moderator temperature are represented.

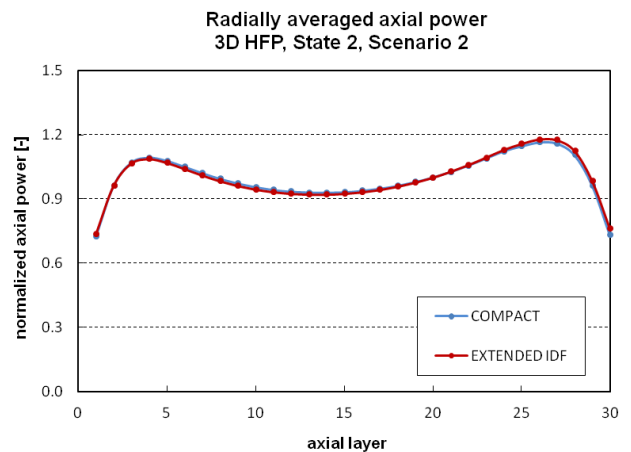


Fig. 10 Axial power distribution at HFP for VVER

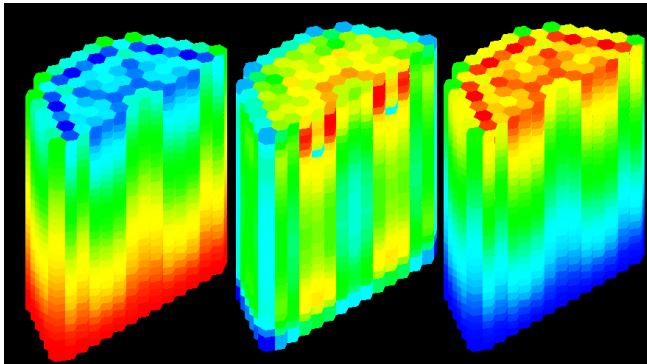


Fig. 11. Distribution of moderator density (l), fuel temperature (c) and moderator temperature (r) at HFP for VVER

2. Transient

Figure 12 shows the predicted time history of total core power. Coupled code results obtained with COBAYA3/FLICA4, COBAYA4/CTF and DYN3D/CTF are compared code-to-code. A significant return to power can be seen, with a maximum of about 70% of the nominal rated power. This power is released mainly in the overcooled sector around the stuck rods locations. The hot assembly is #129, located between the two rods stuck out of the core. Figure 13 compares solutions in the radial power distribution at the time of maximum overcooling when using compact library versus extended with COBAYA4/CTF system. Stuck rods are emphasized in red color and rest of rods in blue. Both libraries are in agreement.

Fig 14. To Fig. 16 show the evolution of the core average Doppler temperature, moderator density and coolant temperature for DYN3D/CTF and COBAYA4/CTF solutions. In all cases the agreement is very good.

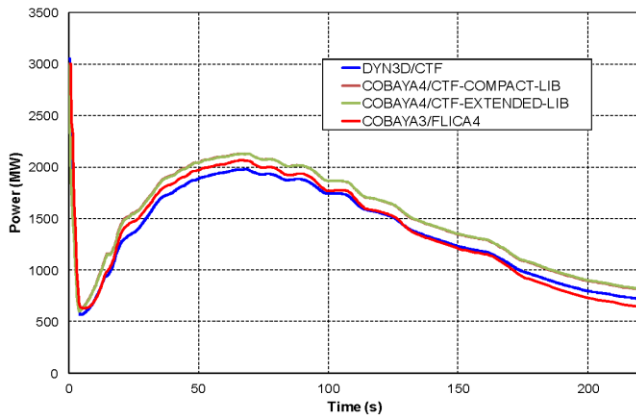


Fig. 12. Power evolution during the MSLB in a VVER

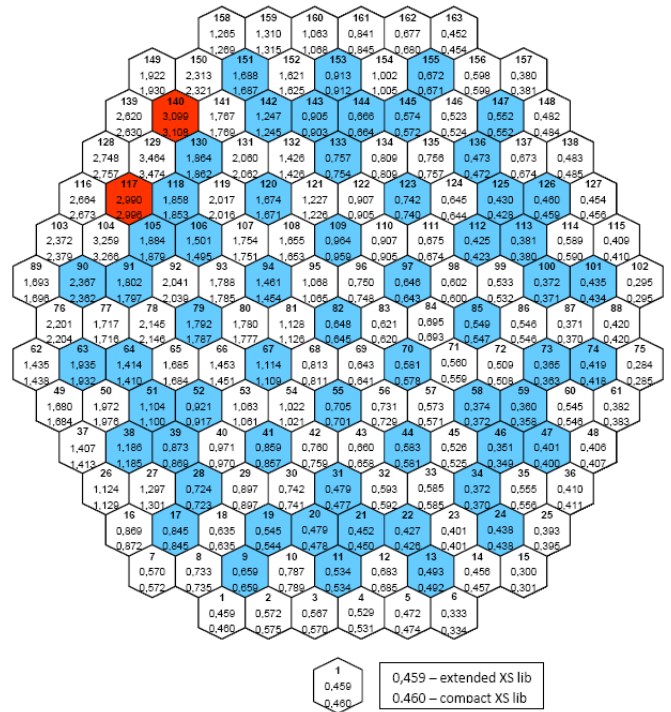


Fig. 13. Radial power distribution during the MSLB in VVER at time of maximum overcooling computed with COBAYA4/CTF with compact and extended libraries

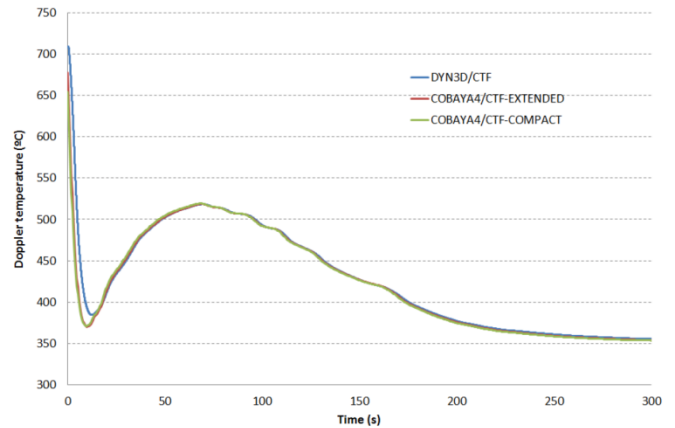


Fig. 14. Core average Doppler temperature evolution during the MSLB in a VVER

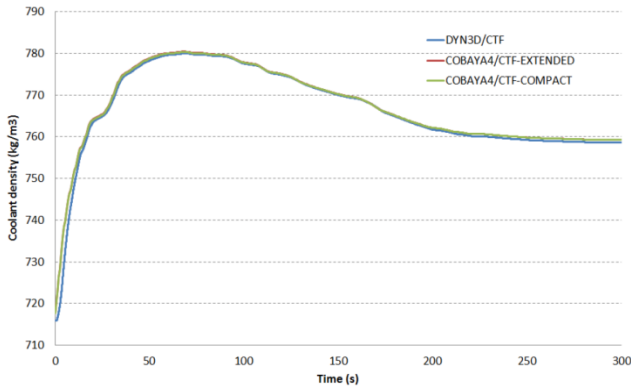


Fig. 15. Core average moderator density evolution during the MSLB in a VVER

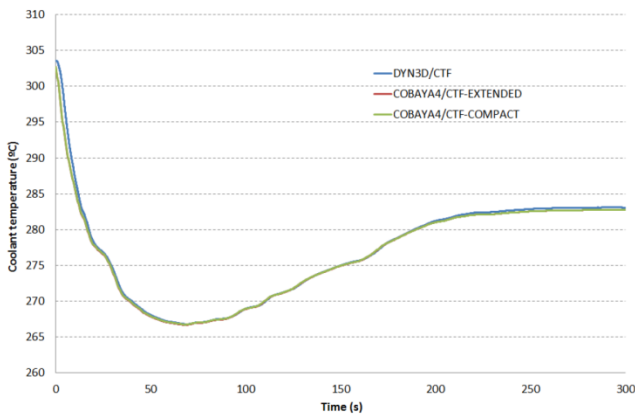


Fig. 16. Core average coolant temperature evolution during the MSLB transient in a VVER

Others results such as comparisons in peak factors, and CFD calculations to study the impact of vessel mixing modeling are included in [Kolev, 2016b].

V. CONCLUSIONS

The coupled system COBAYA4/CTF has been applied to a couple of MSLB transient benchmarks defined in the frame of NURES SAFE project. In PWR, pin-by-pin and nodal solutions were computed using in both cases assembly-based thermal-hydraulic channels. While global parameters, such as the total power or reactivity along the transient, were not very influenced by the neutronics refinement, differences in assembly-averaged peaking factors up to 4% were found between both calculations.

In VVER, COBAYA results are in very good agreement in HZP cases with DYN3D as well as in the transient where power evolution is very similar with other systems like DYN3D/CTF.

Both benchmarks constitute a verification exercise of the new code COBAYA4. This work shows the new capabilities acquired in the code and its great potential as

simulation tool thanks to the work carried out by UPM team during NURES SAFE project.

REFERENCES

- Chanaron, B., Ahnert, C., Crouzet, N., Sanchez, V., Kolev, N., Marchand, O., Kliem, S., Papukchiev, A. "Advanced multi-physics simulation for reactor safety in the framework of the NURES SAFE project" *Annals of Nuclear Energy* **84**, 166 – 177. (2015)
- Chanaron, B., Kliem, S., Bestion, D., Lakehal, D., Crouzet, N. "Overview of the NURES SAFE European Project" *Nucl. Eng. Dsgn.*, submitted (2016)
- Lozano J. A., García-Herranz, N., Ahnert, C., Aragonés, J. M. "The analytic nodal diffusion solver ANDES in multigroups for 3D rectangular geometry: Development and performance analysis" *Annals of Nuclear Energy* **35**(12), 2365-2374. (2008)
- Herrero J.J., Jiménez J., Aragonés J. M., Ahnert C. "Performance of whole core pin-by-pin calculations by domain decomposition through alternate dissections in steady state and transient calculations" *Proc. M&C 2009*, May 3–7, 2009, Saratoga Springs, New York.
- García-Herranz, N., Cuervo, D., Sabater, A., Rucabado, G., Sánchez-Cervera, S., Castro, E. "Multiscale neutronics/thermal-hydraulics coupling with COBAYA4 code for pin-by-pin PWR transient analysis" *Nucl. Eng. Dsgn.*, submitted (2016)
- Salko R. and Avramova M. "CTF Subchannel Thermal-Hydraulics Code (CTF) Theory Manual" CASL-U-2015-0054-000. (2015)
- Sabater, A., Cuervo, D., Sánchez-Cervera, S. "Comparison of subchannel and averaged channel thermal-hydraulic descriptions on coupled pin-by-pin neutronic calculations" *ANS Winter Meeting*, Las Vegas, Nevada, November 6-10, 2016, American Nuclear Society (2016)
- Kozłowski T., Downar T. *OECD/NEA and US-NRC PWR MOX/UO₂ Core Transient Benchmark, Final Specifications*, NEA/NSC/DOC (2003)
- Kliem, S., Kozmenkov, Y., Hadek, J., Perin, Y., Fouquet, F., Bernard, F., Sargeni, A., Cuervo, D., Sabater, A., Sánchez-Cervera, S., García-Herranz, N., Zerkak, O., Ferroukhi, H., Mala, P. "Testing the NURESIM platform on a PWR main steam line break benchmark" *Nucl. Eng. Dsgn.*, submitted (2016)
- Sánchez-Cervera, S., García-Herranz, N., Herrero, J.J. Cabellos, O. "Optimization of multidimensional cross-sections tables for few-group core calculations" *Annals of Nuclear Energy* **69**, 226-237 (2014)
- Kolev, N.P. et al, "VVER-1000 Coolant transient benchmark Phase II (V1000CT-2), Vol.2, Final Specifications of the VVER-1000 MSLB problem", NEA/NSC/DOC 2006(6) © OECD 2010
- Kolev, N.P., Spasov, I., Zheleva, N., Todorova, G., Petrov, N., Ivanov, P., Mitkov, S., Kamenscic, O., Hadek, J., Vyskocil, L., Jimenez, J., Sanchez, V., Sánchez-Cervera, S., Garcia-Herranz, N., Sabater, A. and Cuervo, D. "Higher-

resolution VVER MSLB simulation - Final report”,
NURESAFE D14.41 report, (2016,a)

13. Kolev, N., Spasov, I., Sánchez-Cervera, S., García-Herranz, N., Sabater, A., Cuervo, D., Jiménez, J., Sanchez, V., Vyskocil, L. “Best-estimate simulation of a VVER MSLB core transient using NURESIM platform codes”
Nucl. Eng. Dsgn., submitted (2016,b)